

## Resistivity recovery in cobalt following electron irradiation at 8 K

This article has been downloaded from IOPscience. Please scroll down to see the full text article.

1989 J. Phys.: Condens. Matter 1 9519

(<http://iopscience.iop.org/0953-8984/1/48/002>)

View [the table of contents for this issue](#), or go to the [journal homepage](#) for more

### Download details:

IP Address: 171.66.16.96

The article was downloaded on 10/05/2010 at 21:08

Please note that [terms and conditions apply](#).

## Resistivity recovery in cobalt following electron irradiation at 8 K

S Habtetsion†, H J Blythe†, F Dworschak‡ and U Dedek‡

† Physics Department, The University, Sheffield, UK

‡ Institut für Festkörperforschung der KFA Jülich, FRG

Received 3 April 1989, in final form 18 July 1989

**Abstract.** The recovery of the electrical resistivity of high-purity polycrystalline cobalt and cobalt containing either substitutional impurities or interstitially dissolved carbon is investigated in the temperature range 10–450 K following electron irradiation at 8 K with 3 MeV electrons up to integrated doses of  $2.5 \times 10^{23} \text{ m}^{-2}$ . In pure cobalt a strong stage-I recovery (70–78%) is observed centred at 40 K; this recovery is split into a series of sub-stages. No stage-I<sub>E</sub> recovery has been observed. Stage-II recovery (15–20%) extends from 60 to 220 K and consists of a series of small sub-stages. Stage-III recovery (5–10%) centred at 320 K shifts to lower temperatures with increased dose. The influence of impurities is to suppress partially the stage-I and -III recoveries and to increase that of stage II.

### 1. Introduction

Measurement of the recovery of the electrical resistivity of a metal following low-temperature fast-particle irradiation is the classic technique for the investigation of irradiation damage. Measurements on cubic-structured metals are now of such abundance that in these materials a general classification of the annealing behaviour has been achieved and the principal interest at the moment is focused on the general philosophy of the interpretation [1–3]. At the present time this is not the situation in the hexagonal-close-packed (HCP) structured metals which have not yet been investigated so systematically. One of the reasons for this is probably the difficulty which has existed in the preparation of materials of sufficiently high purity, a criterion of paramount importance in point-defect work. Cobalt is an HCP structure of particular interest since it has a  $c/a$  ratio which is close to the ideal value of  $(8/3)^{1/2}$  and it is also of considerable technological importance. In the past, various authors [4–12] have reported electrical resistivity measurements on irradiated cobalt following low-temperature irradiation. Usually, however, there has been some limitation on the results. Measurements have either been confined to a fairly narrow range of temperature, or a single irradiation dose, or have been made on samples of relatively low purity. In the present work we have investigated high-purity cobalt over a wide range of temperature and doses. We have also investigated the influence of both substitutional and interstitial impurities on the annealing behaviour.

### 2. Experimental procedure

#### 2.1. Sample preparation

The source material for the resistivity measurements was either high-purity Johnson Matthey cobalt with a nominal metallic impurity content of less than 35 PPM or cobalt of

**Table 1.** Impurity content of the samples.

	High-purity cobalt	Low-purity cobalt	Carbon-charged high-purity cobalt
Supplier's analysis (PPM)	Al: 2, Cu: 2, Fe: 1, Ca <1, Mn <1, Mg <1, Si <1, Ag <1	Fe: 180, Ni: 800	
KFA analysis (PPM)	Cu <6, Fe <30 ± 25%	Cu: 6, Si: 20, Fe: 150, Ni: 300, ±25%	1.9 × 10 <sup>3</sup>
$\Gamma = R(273)/R(4.2)$	99	31	4

a lower purity (99.8%) from Goodfellow Advanced Materials; cobalt of two widely differing impurity levels was deliberately selected so as to give us a convenient method of varying the substitutional impurity content. The Johnson Matthey material was originally in sheet form measuring  $40 \times 40 \times 0.5 \text{ mm}^3$ . The Goodfellow material was in the form of foil  $100 \times 100 \text{ mm}^2$  of thickness  $125 \mu\text{m}$ . In order to produce samples which were of suitable thickness for resistivity measurements in our experimental arrangement, the starting material had to be reduced to a final thickness of about  $35 \mu\text{m}$ . This was achieved by so called 'book-rolling', which was performed at the National Physical Laboratories, Teddington. The material was sandwiched between two sheets of stainless steel which were then spot-welded at their edges and then cold-rolled to  $35 \mu\text{m}$ . No intermediate anneal was found to be necessary. Resistance samples (3 cm long, 3.0 mm wide) were cut from these foils. All samples were finally cleaned and annealed for 100 h at 1000 K in palladium-diffused hydrogen in order to remove interstitial carbon and nitrogen. At the end of this anneal, samples were cooled slowly to room temperature in an attempt to minimise the content of the FCC phase; this is inevitably present to some extent in polycrystalline material due to the martensitic transformation which, in cobalt, occurs at about 700 K.

After the purification procedure, some of the samples produced from the Johnson Matthey material were charged with carbon, thus providing us with a comparison of high-purity cobalt with and without interstitial impurity. This was achieved by painting the samples with 'Zaponlack', a commercial hydrocarbon lacquer, sealing them in quartz ampoules under vacuum and annealing for 24 h at 1100 K; the samples were air-cooled to room temperature in an attempt to retain carbon in interstitial solution. At the end of the resistivity measurements, after irradiation and final anneal of the samples, a spectrographic analysis was performed on the actual samples which had been used in the experiment. The metallic impurities were determined using emission spectral analysis and the carbon content of the doped samples was determined from infrared spectroscopy. These analyses were performed by the Central Department for Chemical Analysis of the KFA, Jülich. The results of these analyses are given in table 1 together with the nominal analyses provided by the suppliers.

Residual resistivity ratios for the various samples,  $R(273)/R(4.2) \equiv \Gamma$ , were determined without the application of an external magnetic field. The results of these measurements are included in tables 1 and 2. The highest value of  $\Gamma$ ,  $\sim 99$ , was obtained for the high-purity material, whereas the lower-purity and carbon-doped samples had values of  $\sim 31$  and  $\sim 4$  respectively. In comparison with the values of  $\Gamma$  which are currently obtained for the cubic metals (e.g. for Fe,  $\Gamma \approx 5 \times 10^3$  [3], for Al,  $\Gamma \approx 2 \times 10^4$  [13]) these values are extremely low, although comparable with values obtained for cobalt by other workers [6, 8, 9, 11, 12]. In view of these low values, it was decided to perform TEM measurements

**Table 2.** Sample data. Here,  $\Gamma = R(273)/R(4.2)$  is the residual resistivity ratio,  $\Phi_t$  is the total integrated dose (accurate to within  $\pm 5\%$ ),  $\Delta\rho_0$  the radiation-induced resistivity, and  $\rho_0$  the residual resistivity measured at 4.2 K in zero applied field.

Sample No	Sample type <sup>a</sup>	$\Gamma$	$\Phi_t (\times 10^{22} \text{ m}^{-2})$	$\Delta\rho_0 (\times 10^{-11} \Omega \text{ m})$	$\rho_0 (\times 10^{-11} \Omega \text{ m})$
1	HP + C	3.6	1.0	20.06	2236
2	LP	31.3		17.67	192.7
3	HP	93.0		21.79	62.84
4	LP	31.3	8.9	104.8	192.7
5	HP	98.1	6.7	104.9	59.54
6	HP	90.0		105.5	64.92
7	HP	94.1	24.5	321.9	62.07
8	LP	30.9		316.6	195.6
9	HP + C	3.4		351.8	2440
10	LP	31.6	7.8	98.97	190.8
11	HP	99.0	6.0	97.25	59.02
12	HP + C	3.9	6.0	104.1	2033

<sup>a</sup> HP, high-purity cobalt; LP, low-purity cobalt; HP + C, high-purity cobalt charged with carbon.

on some of the samples after they had been rolled to their final thickness and annealed. As was expected, this revealed a very high density of dislocations and stacking faults which we attribute to the martensitic phase change; the dislocation density was typically of the order  $10^{13} \text{ m}^{-2}$ . However, no systematic investigation of the various samples was undertaken. It would perhaps seem that in polycrystalline cobalt, residual resistivity measurements are not a very sensitive indicator of sample purity.

## 2.2. Sample irradiation

Twelve samples were mounted onto a sample holder which fitted into an irradiation cryostat; details of this are given in reference [14]. The experimental arrangement enabled up to three samples to be irradiated simultaneously. The irradiations were performed using a Van de Graaff accelerator and 3 MeV electrons. Sample temperature during irradiation was monitored via the electrical resistivity of one of the high-purity samples in the sample holder; this temperature determination was performed at the beginning of the irradiation before any appreciable defect concentration had been built up. A sample temperature of about 8 K was maintained throughout the irradiation with a dose rate of  $6 \times 10^{17} \text{ e}^- \text{ m}^{-2} \text{ s}^{-1}$ , accurate to within  $\pm 5\%$ . The integrated doses and the radiation-induced resistivities obtained for the different samples are given in table 2.

## 2.3. Measuring technique

All resistivity measurements were performed at 4.2 K using a standard four-terminal method. In a preliminary measurement it had been established that applying an external magnetic field during measurement of the resistance resulted in negligible decrease in scatter of the data. All measurements were thus subsequently made without an applied field; the reproducibility of resistivity determinations made in this manner was better than  $10^{-12} \Omega \text{ m}$ . In order to determine the shape factor,  $k$ , we used the relationship

$$k = \rho^{\text{Co pure}}(273)/[R(273) - R(4.2)]$$

where  $R(273)$  and  $R(4.2)$  are the electrical resistance of the sample at 273 K and 4.2 K

respectively. For  $\rho^{\text{Co}_{\text{pure}}}$  (273) we assumed a value of  $5.2 \times 10^{-8} \Omega \text{ m}$  [15]. An estimate of the carbon content of the samples was made from the values obtained for the residual electrical resistivity (table 2). Assuming a value of  $4.4 \times 10^{-6} \Omega \text{ m/at. \%}$  for the specific resistivity of carbon in cobalt [16] we obtain a concentration of about 900 PPM by weight. This is roughly half the value obtained from the chemical analysis and suggests that only half the carbon in the samples was in solution.

#### 2.4. Annealing procedure

After the irradiation the samples were isochronally annealed for 15 min periods with temperature increments of  $\Delta T = 1 \text{ K}$  for the range 4–30 K and  $\Delta T/T = 0.03$  for higher temperatures, and the recovery of the radiation-induced residual resistivity increase,  $\Delta\rho$ , was measured. Temperatures in the range 4–500 K could be attained by raising the sample holder into one of three copper blocks mounted vertically above one another and contained within the cryostat; details are given elsewhere [17]. Since the anneals were carried out in a helium atmosphere and the required temperature of the appropriate copper block was stabilised before insertion of the sample holder, sample temperatures could be stabilised within a few seconds and the temperature stability of the blocks was of the order of 0.1%.

### 3. Experimental results

#### 3.1. High-purity samples

Figure 1(a) shows the dose dependence of the isochronal recovery of high-purity cobalt in the temperature range 5–470 K; figure 1(b) gives the same results in a differential isochronal plot. In agreement with previous authors [4–11] we designate the recovery stage which occurs below about 60 K as the stage-I recovery, the recovery which occurs between 60 and 220 K as stage II and that which is centred at 300 K as the stage-III recovery. Total recovery in stage I varies from 77% for the low-dose sample to 70% for the high-dose sample. In stage II, corresponding values are 17% to 19% and in stage III, 5% to 11%. The stage-I recovery is split into a series of sub-stages. Stage  $I_A$ , which occurs at about 15 K, both decreases and shifts to higher temperatures with increasing dose. Stage  $I_C$ , at 33 K, decreases with increasing dose whereas for the sub-stages  $I_{D1}$ , at 42 K, and  $I_{D2}$ , at 53 K, the recoveries are almost independent of dose. Stage  $I_B$ , which has been observed by other workers [7], is only seen here as a low-temperature shoulder on stage  $I_C$ . No evidence is found for a recovery stage at 60 K which has previously been observed [7, 11] and designated as stage  $I_E$ . Recovery stage II is composed of a large number of small recoveries which, with the exception of a recovery peak at 169 K characterised by an increase of amplitude with increasing dose, are almost dose-independent. A stage-III recovery is observed which is characterised by an increase in amplitude and a shift of maximum to lower temperatures with increasing dose (figure 2).

#### 3.2. Carbon-doped samples

Figures 3(a) and (b) show the dose dependence of the isochronal recovery and the corresponding differential recovery for the high-purity cobalt samples charged with carbon. In all the carbon-charged samples recovery stage  $I_A$  is strongly suppressed and

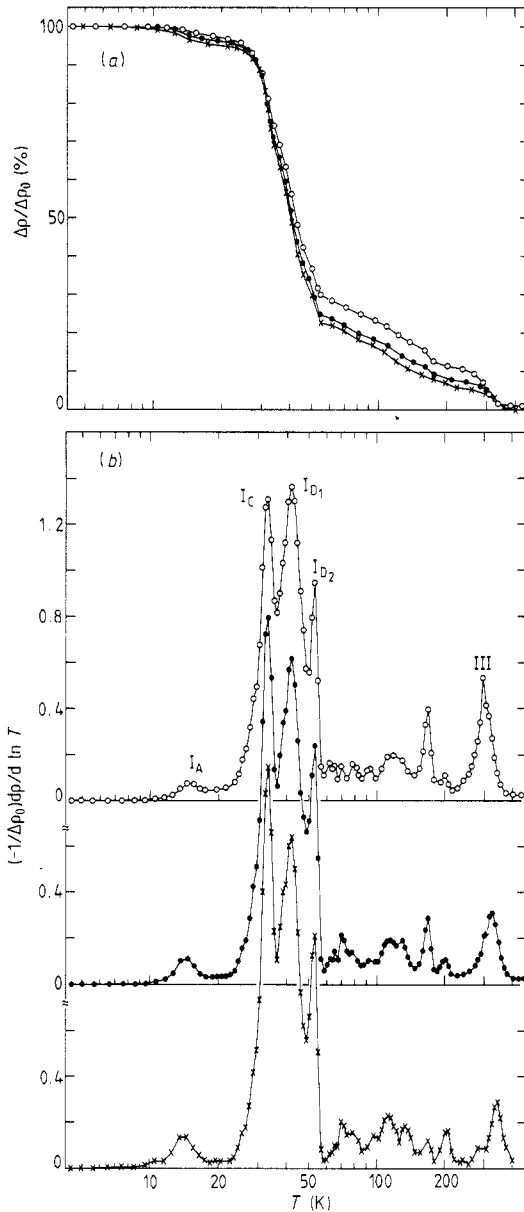


**Figure 1.** (a) Dose dependence of the isochronal recovery of high-purity cobalt after 3 MeV electron irradiation at 8 K. Not all data points are shown.  $\circ$ ,  $\Delta\rho_0 = 321.9 \times 10^{-11} \Omega \text{ m}$  (sample No 7);  $\bullet$ ,  $\Delta\rho_0 = 104.9 \times 10^{-11} \Omega \text{ m}$  (sample No 5);  $\times$ ,  $\Delta\rho_0 = 21.8 \times 10^{-11} \Omega \text{ m}$  (sample No 3). (b) Same results in a differential isochronal plot.

it is no longer possible to resolve the three sub-stages  $I_C$ ,  $I_{D1}$  and  $I_{D2}$ . There is an additional strong recovery at 112 K and the pronounced recovery observed at 169 K in high-purity samples is enhanced and supplemented by an additional peak at slightly higher temperatures. It is interesting to note that at about 280 K, in all carbon-charged samples, there is a negative recovery (figure 3(b)). Stage III is strongly suppressed and at 400 K a very rapid recovery sets in.

### 3.3. Low-purity samples

In the samples containing substitutional impurities (figures 4(a) and (b)), stage  $I_A$  seems to be relatively unaffected as compared with the behaviour of the carbon-doped samples.

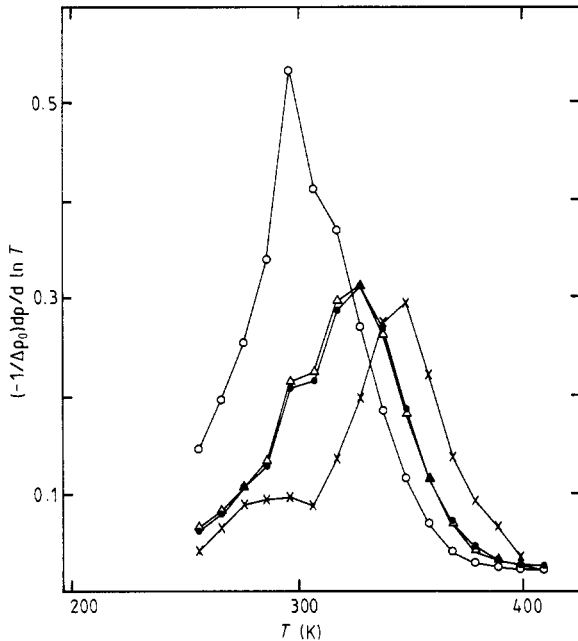


**Figure 2.** Differential plot of the isochronal recovery stage III for high-purity cobalt after 3 MeV electron irradiation at 8 K.  $\circ$ ,  $\Delta\rho_0 = 321.9 \times 10^{-11} \Omega \text{ m}$  (sample No 7);  $\triangle$ ,  $\Delta\rho_0 = 97.3 \times 10^{-11} \Omega \text{ m}$  (sample No 11);  $\bullet$ ,  $\Delta\rho_0 = 104.9 \times 10^{-11} \Omega \text{ m}$  (sample No 5);  $\times$ ,  $\Delta\rho_0 = 21.8 \times 10^{-11} \Omega \text{ m}$  (sample No 3).

However, this may well be due to the fact that the impurity level is much greater in the carbon-charged samples than in the low-purity material. The three sub-stages  $I_C$ ,  $I_{D1}$  and  $I_{D2}$  are also still resolved but reduced in amplitude compared with the high-purity results. In addition to the suppressed 112 K and 169 K peaks, several recovery processes occur in the range of stage II whereas the stage-III recovery is relatively unaffected.

### 3.4. Unirradiated samples

In an attempt to distinguish between the effects of radiation-induced defects and that of interstitial carbon in the samples, three unirradiated carbon-charged samples were measured from room temperature up to 700 K in an identical annealing programme ( $\Delta T/T = 0.03$ ) to that employed for the irradiated samples. As a reference, an unirradiated high-purity sample was also measured at the same time. The results of these measurements are shown in figure 5. In the carbon-charged sample a strong recovery occurs centred at 500 K together with a smaller recovery at 650 K. In contrast to this behaviour, the high-purity sample shows no recovery at 500 K but a slight recovery at temperatures above 600 K.

## 4. Discussion

### 4.1. Previous work

There have been several earlier reports of measurement of the recovery of the electrical resistivity in low-temperature irradiated cobalt. Coltman *et al* [4] reported measurements made on high-purity polycrystalline material ( $\Gamma \approx 113$ ) after thermal-neutron damage at 3.6 K producing a resistivity increase of  $7.9 \times 10^{-11} \Omega \text{ m}$ ; these recovery measurements extended up to 300 K when 91% recovery had occurred. The differential recovery spectrum was very similar to that found for the present high-purity material. Maury *et*

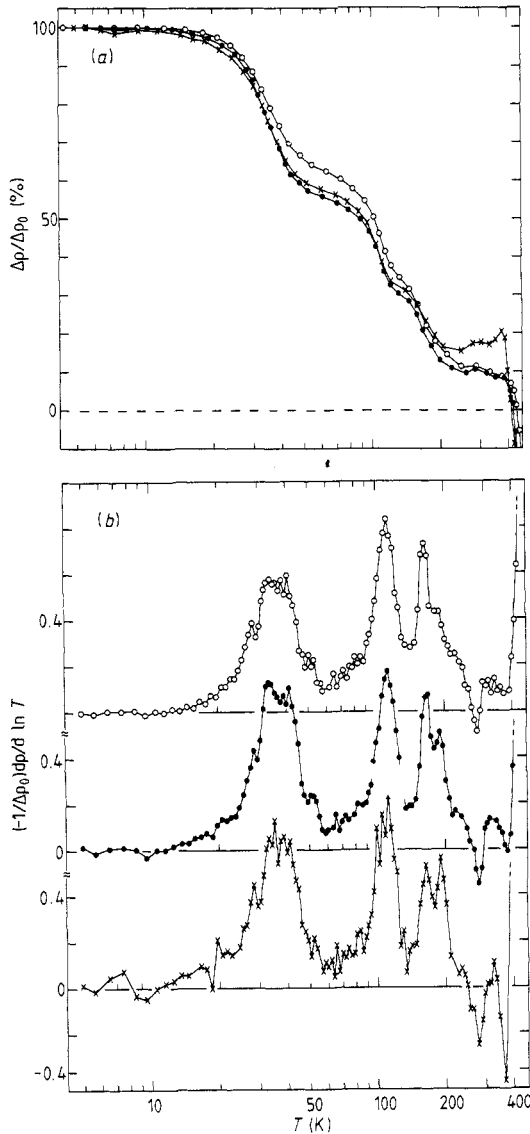


**Figure 3.** (a) Dose dependence of the isochronal recovery of high-purity cobalt doped with carbon after 3 MeV electron irradiation at 8 K. Not all data points are shown.  $\circ$ ,  $\Delta\rho_0 = 351.8 \times 10^{-11} \Omega \text{ m}$  (sample No 9);  $\bullet$ ,  $\Delta\rho_0 = 104.1 \times 10^{-11} \Omega \text{ m}$  (sample No 12);  $\times$ ,  $\Delta\rho_0 = 20.1 \times 10^{-11} \Omega \text{ m}$  (sample No 1). (b) Same results in a differential isochronal plot.

*al* [8–10] have investigated the anisotropy of radiation damage and its recovery in cobalt single crystals ( $\Gamma \approx 10\text{--}20$ ) following low-temperature electron irradiation. The main recovery was found to occur at about 33 K (stage  $I_C$ ) and, at low electron energies, this could be resolved into two distinct sub-peaks, the magnitude of which depended upon the crystallographic orientation.

Cope *et al* [7] have investigated the recovery of the electrical resistivity in cobalt following 3 MeV electron irradiation at 20 K to doses of between  $10^{21}$  and  $10^{22} \text{ m}^{-2}$ . Although the measurements extended over the temperature range 20–300 K, almost all the recovery seemed to have occurred below 90 K. A prominent stage I was observed, including a stage  $I_E$  recovery. This latter stage, at 70 K, was displaced in agreement with second-order kinetics. Dander and Schaefer [11] have also reported measurements in cobalt following 5 K irradiation with 3 MeV electrons to doses between  $10^{22}$  and  $8.6 \times 10^{22} \text{ m}^{-2}$  corresponding to resistivity increases of  $21 \times 10^{-11}$ – $239 \times 10^{-11} \Omega \text{ m}$



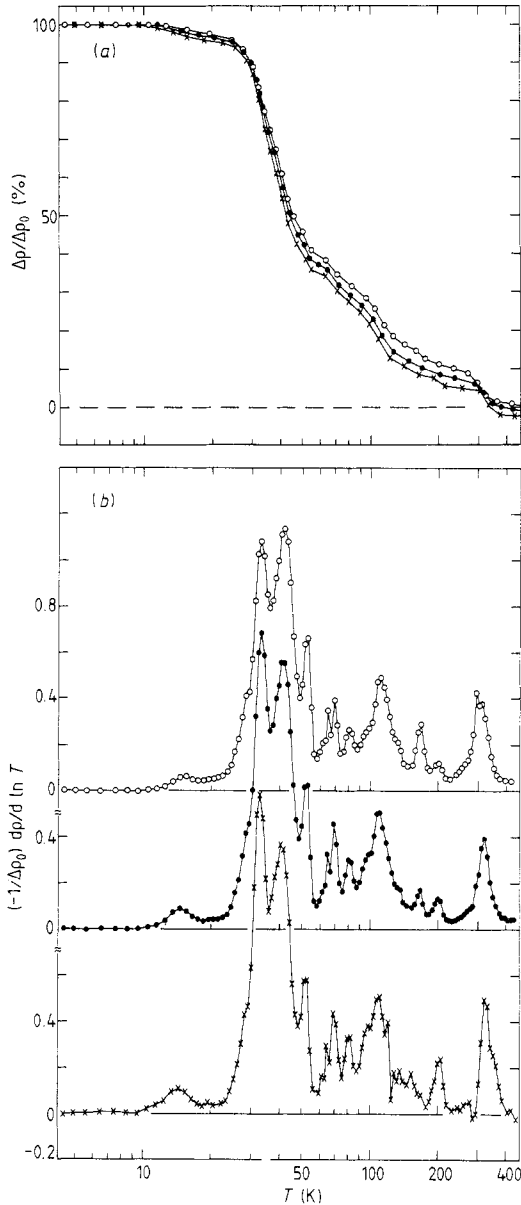


**Figure 4.** (a) Dose dependence of the isochronal recovery of cobalt containing substitutional impurities after 3 MeV electron irradiation at 8 K. Not all data points are shown. ○,  $\Delta\rho_0 = 316.6 \times 10^{-11} \Omega \text{ m}$  (sample No 8); ●,  $\Delta\rho_0 = 104.8 \times 10^{-11} \Omega \text{ m}$  (sample No 4); ×,  $\Delta\rho_0 = 17.7 \times 10^{-11} \Omega \text{ m}$  (sample No 2). (b) Same results in a differential isochronal plot.

respectively. The temperature range investigated extended from 15–550 K. In this work, a large number of recovery processes was observed; this was attributed by the authors, to some extent, to the relatively low purity of their material ( $\Gamma \approx 50$ –100). However, the recovery stage  $I_E$  was apparently detected and exhibited a dose-dependent shift, although the recovery at 15 K was absent. More recently Kobiyama and Takamura [12], in a general investigation of HCP metals after fast-neutron irradiation at 5 K, have observed in polycrystalline cobalt ( $\Gamma \approx 34$ ) a recovery spectrum similar to that observed in the present work. However, stage I could not be resolved into distinct sub-stages, nor was recovery stage  $I_E$  observed.

Ehrhart and Schönfeld [18] measured the diffuse scattering of x rays, the change of lattice parameter and the change of the electrical resistivity of pure cobalt single crystals

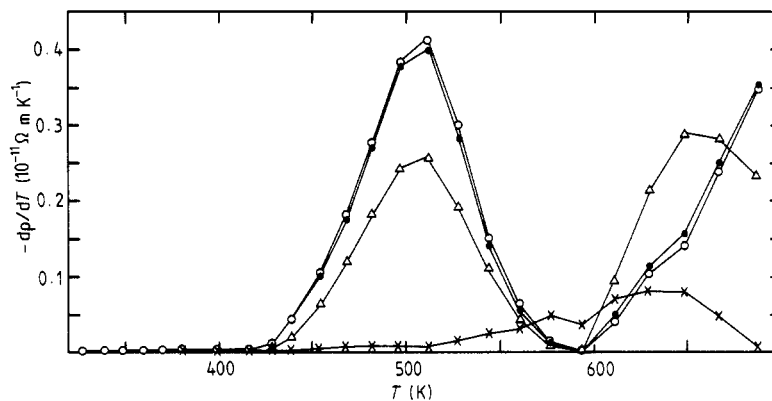


**Figure 5.** Differential isochronal recovery in the temperature range 300–700 K of un-irradiated high-purity cobalt and cobalt charged with carbon. The residual resistivities of the samples prior to anneal were:  $\circ$ , high-purity cobalt + C,  $\rho_0 = 628.1 \times 10^{-11} \Omega \text{ m}$ ;  $\triangle$ , high-purity cobalt + C,  $\rho_0 = 528.1 \times 10^{-11} \Omega \text{ m}$ ;  $\bullet$ , high-purity cobalt + C,  $\rho_0 = 604.7 \times 10^{-11} \Omega \text{ m}$ ;  $\times$ , high-purity cobalt,  $\rho_0 = 54.3 \times 10^{-11} \Omega \text{ m}$ .

after 3 MeV electron irradiation at 4.5 K. From an analysis of their data, the authors calculated  $\rho_{\text{FP}} = (16 \pm 5) \times 10^{-8} \Omega \text{ m/at.}\%$ . In spite of the high defect concentrations (300 at. ppm), no large self-interstitial clusters were formed at the end of stage-I annealing (the average number of self-interstitials per cluster was estimated to be about 1.5).

There have been several computer modelling investigations of point defects in the HCP metals [19–22]; these have been critically reviewed by Bacon [23]. All the simulations indicate that the self-interstitial in the HCP metals has a variety of stable forms, such that the stable defect could be different in different metals depending on the  $c/a$  ratio. In a recent review article, Frank [25] has discussed the problem of damage recovery in the HCP metals and compared the prediction of computer calculations with a wide range of experimental data.

## 4.2. Present work

**4.2.1. Stage I.** A striking feature of the stage-I recovery in cobalt is that the main recovery is resolved into three distinct, but very close, sub-stages. We have classified these sub-stages in agreement with the work of Sulpice [6]. Since there is no apparent shift in the maxima of the differential recoveries with dose, we have concluded that they are first-order processes and, assuming a value of  $K_0 \sim 10^{13} \text{ s}$ , have attempted to fit them with a standard theoretical expression [25] assuming a single, discrete activation energy. However, it was found that the widths of these theoretical curves were, in all cases, a factor of about three too small. A similar disagreement has also been found for close-pair-recovery stage  $I_C$  in other metals, e.g. in electron-irradiated platinum [26].

A further important feature of stage I is the absence of a stage- $I_E$  recovery. In an annealing spectrum this is usually identified as that recovery which, at the end of stage I, exhibits a shift to lower temperatures with increasing dose, this being characteristic of a long-range migration. However, a stage  $I_E$ , together with dose-dependent shift, has been reported, by Cope *et al* [7] and by Sulpice *et al* [6] after doses of  $1.6 \times 10^{21} \text{ m}^{-2}$  and  $1.5 \times 10^{22} \text{ m}^{-2}$  respectively. Since the lowest dose in the present work was  $1.0 \times 10^{22} \text{ m}^{-2}$  it would be argued that the absence of stage  $I_E$  in the present work is due to the higher doses used; reasons often given for the absence of stage  $I_E$  are high radiation dose or low

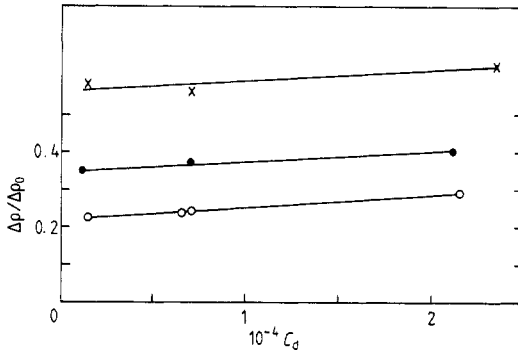


**Figure 6.** Normalised defect retention after stage-I anneal plotted as a function of the total radiation-induced defect concentration,  $C_d$ .  $\times$ , high-purity cobalt + C,  $\Delta\rho_0 = (20.1\text{--}351.8) \times 10^{-11} \Omega \text{ m}$ ;  $\bullet$ , cobalt with substitutional impurity,  $\Delta\rho_0 = (17.7\text{--}316.6) \times 10^{-11} \Omega \text{ m}$ ;  $\circ$ , high-purity cobalt,  $\Delta\rho_0 = (21.8\text{--}321.9) \times 10^{-11} \Omega \text{ m}$ .

sample purity. On the other hand, Sulpice *et al* [6] report a resistivity increase of about  $26 \times 10^{-11} \Omega \text{ m}$  after a 1.4 MeV electron irradiation up to  $1 \times 10^{22} \text{ m}^{-2}$ , whereas, in the present experiment, the resistivity increase amounted to only  $20 \times 10^{-11} \Omega \text{ m}$  after a dose of  $1 \times 10^{22} \text{ m}^{-2}$  of 3 MeV electrons. Consequently, the defect concentrations did not differ much in these two experiments.

In carbon-doped samples, recovery stage  $I_A$  is completely suppressed and all other sub-stages are strongly attenuated. This is not unexpected and can be attributed to the trapping of self-interstitials at interstitial carbon atoms. It is interesting to note that in the carbon-free, low-purity cobalt sample, stage  $I_A$  is relatively unaffected, although the other sub-stages are somewhat reduced. This may be due to the fact that a lower level of impurity in the low-purity sample than in the carbon-doped ones results in a larger self-interstitial–impurity atom separation or that substitutional impurities (in this case mainly nickel, with a negative size factor) are less effective in interstitial retention.

The influence of purity and defect concentration upon the damage remaining after stage-I annealing is shown in figure 6. Here we have plotted the normalised defect retention after stage I as a function of the total radiation-induced defect concentration. We may make the following observations: (i) defect retention increases with increasing impurity content for all initial defect concentrations; (ii) defect retention increases with increasing initial defect concentration, as can be seen from the positive slopes of all three lines.

These results are in accord with the assumption of the free migration of a self-interstitial in stage I (according to either the one- or the two-interstitial annealing model [1, 2]) since:

(i) as a migrating self-interstitial that escapes recombination is trapped by impurity atoms, more damage is retained after stage I;

(ii) with increasing defect concentration, we have increasing defect retention due to cluster formation; this occurs in samples of all purities. However, in cobalt, defect clustering does not seem to be an important characteristic since the positive slopes (figure 6) are very small. This observation is in good agreement with the results of Ehrhart and Schönfeld [18].

**4.2.2. Stage II.** Historically, stage II is assigned to the recovery region situated between stage I and stage III. In a pure metal, in either of the two annealing models [1, 2], recovery in this stage is generally attributed to the decay of small interstitial clusters formed during stage I. In impure metals or dilute alloys the recovery in stage II is generally attributed to the rearrangement of self-interstitial–impurity complexes or the de-trapping of self-interstitials from impurity traps. In the present work the dilute

cobalt-carbon sample exhibits recovery stages at 112, 169 and 190 K. Since carbon is the dominant impurity it seems reasonable to attribute these recovery stages to the presence of carbon, i.e. to self-interstitial-carbon complexes. However, two of the recovery stages also occur in the low-purity and high-purity material. The 112 K stage is independent of dose and increases with impurity concentration, whereas the 169 K stage increases with increasing dose and is largest in the carbon-doped material. Without further information on the dependence of these peaks on carbon and on dose it seems premature to assign specific recovery models to these recovery stages.

In order to show the influence of sample purity on recovery, in figure 7(a) we have re-plotted the isochronal recovery for the three different types of sample following irradiation to almost equal doses. Figure 7(b) shows the corresponding differential curves. A clear feature of the results (figure 7(a)) is the suppression of recovery which occurs in the impure samples, although above about 110 K the curves for the high- and low-purity cobalt are almost coincident. This suggests that the substitutional impurities nickel and iron are unable to trap intrinsic defects above 110 K.

*4.2.3. Stage III.* In the high-purity cobalt sample, the stage-III recovery (between 300 and 350 K) exhibits the classic shift of peak to lower temperatures with increasing dose (figure 2), which is characteristic of the long-range migration of a defect. This peak shift is less prominent in the low-purity cobalt sample and is practically absent in the carbon-doped cobalt. The recovery is reduced in carbon-doped cobalt but enhanced in the low-purity material.

If we adopt the viewpoint of a one-interstitial model, we should interpret this stage as being due to the long-range migration of vacancies. The decrease in the anneal observed in carbon-doped samples could then be due to vacancy retention at interstitial carbon sites. Alternatively, according to the two-interstitial model this stage would correspond to the migration of the second and stable interstitial type, according to Frank [24] the  $B_0$  configuration. The slight increase in the recovery in samples with substitutional impurity could then be explained by additional decay of the interstitial-impurity cluster remaining over from stage II. In the carbon-doped samples, interstitial retention at carbon atoms reduces the recovery.

An unusual feature of all the carbon-doped samples is the negative anneal which occurs at about 270 K. A similar anneal has been observed in dilute CuBe alloys [27]. This effect could possibly be explained in the present results by the formation of a carbon-intrinsic defect cluster of such a configuration that its specific resistivity is well below that of the sum of the individual defects. On anneal to higher temperature, the very rapid rise in the recovery of the carbon-doped sample is attributed to the precipitation of carbon from solid solution. This is confirmed by a comparison with the behaviour of an unirradiated high-purity and the unirradiated carbon-doped samples (figure 5). The slight recovery that occurs in both types of unirradiated sample may be due to the elimination of cold-work introduced into the samples during mounting in the sample holder.

## 5. Summary

In this paper we have reported on the recovery of the electrical resistivity of high-purity and impurity-doped cobalt following low-temperature electron irradiation.

Stage I (12–60 K) in high-purity cobalt is characterised by being split into a series of sub-stages centred at 15 K ( $I_A$ ), 33 K ( $I_C$ ), 42 K ( $I_{D1}$ ) and 52 K ( $I_{D2}$ ). Since there is no

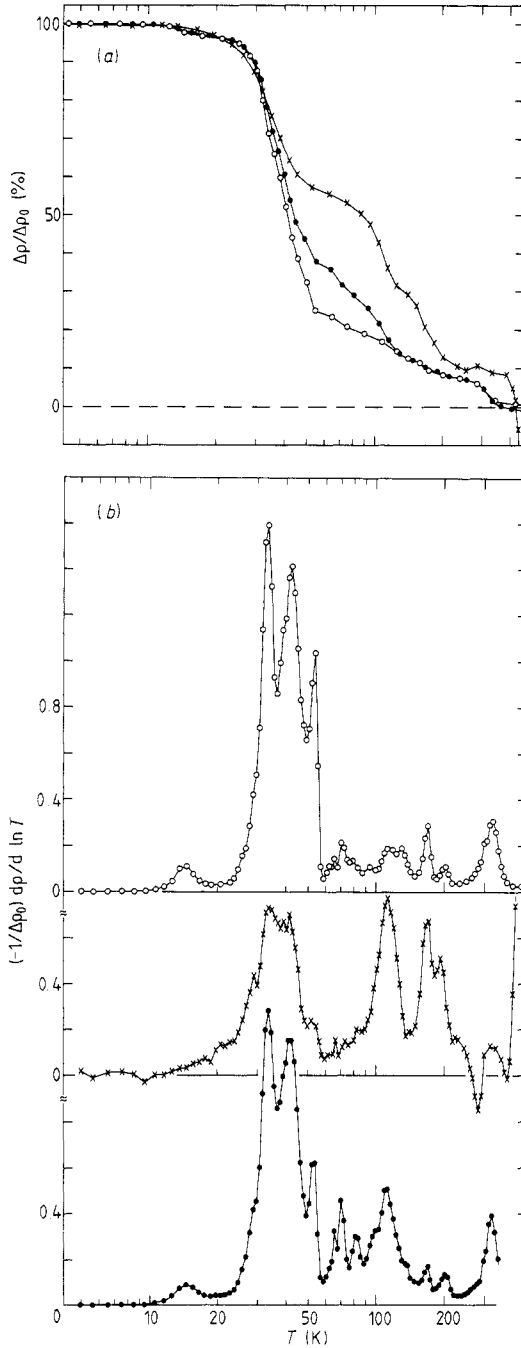


**Figure 7.** (a) Purity dependence of the isochronal recovery of cobalt after 3 MeV electron irradiation at 8 K. Not all data points are shown.  $\circ$ , high-purity cobalt,  $\Delta\rho_0 = 104.9 \times 10^{-11} \Omega \text{ m}$  (sample No 5);  $\bullet$ , cobalt with substitutional impurities  $\Delta\rho_0 = 104.8 \times 10^{-11} \Omega \text{ m}$  (sample No 4);  $\times$ , high-purity cobalt + C,  $\Delta\rho_0 = 104.1 \times 10^{-11} \Omega \text{ m}$  (sample No 12). (b) Same results in a differential isochronal plot.

shift in the maxima of the differential recoveries with dose we have concluded that they are first-order processes. It has, however, not been possible to fit these recoveries theoretically by assuming single, discrete activation energies. A further feature is the absence of a stage- $I_E$  recovery, suggesting that free migration in this stage is suppressed; this may be due either to low sample purity or high radiation dose. In this context, further

measurements are planned on material irradiated to very low doses. The influence of interstitial carbon on the stage-I recovery is the complete suppression of  $I_A$  and strong attenuation of other sub-stages such that they can no longer be resolved. Substitutional impurities, predominantly nickel and iron, only slightly suppress  $I_A$ , although other sub-stages are even more strongly attenuated.

Stage II (70–220 K) in pure cobalt is more or less continuous and consists of a series of weak recoveries with pronounced sub-stages at 112 and 169 K. Interstitial and substitutional impurities increase the recovery in this stage and introduce new recoveries. The sub-stages at 112 and 169 K are strongly increased in the carbon-charged samples and may possibly be attributed to the dissociation of self-interstitial–impurity complexes.

Stage III (300–350 K) in high-purity cobalt exhibits a shift to lower temperatures with increasing dose; this is characteristic of a freely migrating defect. Nickel and iron impurities have little influence on this recovery, whereas interstitial carbon suppresses it strongly.

### Acknowledgment

We would like to thank colleagues at the Max-Planck-Institut für Metallforschung, Stuttgart, for the use of their extensive materials preparation facilities. One of us (SH) would like to thank the Ethiopian Government and Addis Ababa University for sponsoring the study leave and the UNDP for financial assistance. Financial support from the Science and Engineering Research Council is also acknowledged.

### References

- [1] Seeger A 1980 *Proc. R. Soc. London A* **371** 165
- [2] Schilling W, Ehrhart P and Sonnenberg K 1976 *Fundamental Aspects of Radiation Damage in Metals* vol 1 ed. M T Robinson and F W Young Jr p 470
- [3] Takaki S, Fuss J, Kugler H, Dedek U and Schultz H 1983 *Radiat. Effects* **79** 87
- [4] Coltman R R, Klabunde C E and Redman J R 1967 *Phys. Rev.* **150** 715
- [5] Sulpice G 1968 *PhD Thesis* Grenoble
- [6] Sulpice G, Minier C, Moser P and Bilger H 1968 *J. Physique* **29** 253
- [7] Cope H, Sulpice G, Minier C, Bilger H and Moser P 1970 *Vacancies and Interstitials in Metals*, Jülich eds. A Seeger, D Schumacher, W Schilling and J Diehl (Amsterdam: North-Holland) p 792
- [8] Maury F, Roux G, Vajda P, Minier C, Lucasson A and Lucasson P 1970 *Crystal Lattice Defects* **1** 361
- [9] Maury F, Vajda P, Lucasson A and Lucasson P 1973 *Phys. Rev.* **B 8** 5496
- [10] Maury F, Vajda P, Lucasson A and Lucasson P 1973 *Phys. Rev.* **B 8** 5506
- [11] Dander W and Schaefer H-E 1977 *Phys. Status Solidi b* **80** 173
- [12] Kobiyama M and Takamura S 1985 *Radiat. Effects* **84** 161
- [13] Bartels A, Dimitrov C, Dimitrov O and Dworschak F 1982 *J. Phys. F: Met. Phys.* **12** 2483
- [14] Schroeder H and Schilling W 1976 *Radiat. Effects* **30** 243
- [15] Landolt Börnstein *New Series* 1982 Group III vol 15 (Berlin: Springer)
- [16] Swartz J C 1971 *J. Appl. Phys.* **42** 1334
- [17] Schroeder H 1975 *KFA Jülich Report* No 1166
- [18] Ehrhart P and Schönfeld B 1982 *Point Defects and Defect Interactions in Metals* ed. J Takamura, M Doyama and M Kiritani (Tokyo: University of Tokyo Press) p 47
- [19] Beeler J R and Beeler M F 1981 *Interaction Potentials and Crystalline Defects* ed. J K Lee (New York: AIME) p 141
- [20] Fuse M 1985 *J. Nucl. Mater.* **136** 250
- [21] Johnson R A and Beeler J R 1981 *Interaction Potentials and Crystalline Defects* ed. J K Lee (New York: AIME) p 165
- [22] Foster A H, Harder J M and Bacon D J 1987 *Mater. Sci. Forum* **15–18** 849

- [23] Bacon D J 1988 *J. Nucl. Mater.* **159** 176
- [24] Frank W 1988 *J. Nucl. Mater.* **159** 122
- [25] Damask A C and Dienes G J 1967 *Point Defects in Metals* (London: Gordon & Breach)
- [26] Dibbert H J, Sonnenberg K, Schilling W and Dedek U 1972 *Radiat. Effects* **15** 115
- [27] Schilling W, Burger G, Isebeck K and Wenzl H 1970 *Vacancies and Interstitials in Metals* ed. A Seeger, D Schuhmacher, W Schilling and J Diehl (Amsterdam: North-Holland) p 255